Reduced domain wall pinning in ultrathin Pt/$Co_{100-x}B_x$/Pt with perpendicular magnetic anisotropy

R. Lavrijsen,[1,a)] G. Malinowski,[1] J. H. Franken,[1] J. T. Kohlhepp,[1] H. J. M. Swagten,[1] B. Koopmans,[1] M. Czapkiewicz,[2] and T. Stobiecki[2]
[1]*Department of Applied Physics, Center for NanoMaterials and COBRA Research Institute, Eindhoven University of Technology, P.O. Box 513, 5600 MB Eindhoven, The Netherlands*
[2]*Department of Electronics, AGH University of Science and Technology, 30-059 Krakow, Poland*

(Received 16 October 2009; accepted 9 December 2009; published online 11 January 2010)

We have studied the magnetization reversal process in perpendicularly magnetized ultrathin Pt/$Co_{100-x}B_x$/Pt films by means of magneto-optical magnetometry and microscopy. The addition of boron enhances the effective Barkhausen volume indicating a decrease in domain-wall pinning site density and/or strength. This potentially reduces the field and critical current-density for domain-wall depinning/motion, indicating that perpendicularly magnetized Pt/$Co_{100-x}B_x$/Pt could be an interesting candidate for domain-wall motion studies and applications. © *2010 American Institute of Physics*. [doi:10.1063/1.3280373]

Magnetic domain walls (DW) in magnetic nanowires have attracted much attention recently due to their application in field- and current-induced DW logic and magnetic memory devices.[1,2] Most of the reported results have been obtained on systems with an in-plane magnetization and low magnetocrystalline anisotropy, such as permalloy. These systems exhibit relatively complex and wide DW structures in which the spin structure strongly influences the DW's dynamics.[1,3,4] Moreover, the possible transformation of the DW structure during its motion further complicates the physical interpretation of the experiments and hinders a reliable control of the DW propagation. A promising way to circumvent these difficulties reside in the use of ultrathin films exhibiting a high perpendicular magnetic anisotropy (PMA) resulting in a well-defined out-of-plane easy axis. The high PMA results in narrow, robust, and simple Bloch DWs for which current-induced DW motion/depinning is predicted to be efficient[5,6] and reported to show current-induced DW depinning.[7–11]

Although this seems a promising step toward controlled current-induced DW motion, it has been shown that field- and current-induced DW motion in these systems is hindered by a high areal density of DW pinning sites. This is due to the intrinsic properties of the ultrathin and high PMA films, in which narrow Bloch DWs are very sensitive to small local variations in the magnetic/structural properties.[8,12] Thereby, these systems are prone to thermal activation, resulting in a stochastic motion of the DW which prevents reliable control over the DW, a prerequisite for DW based applications. However, progress has been made showing high current-induced DW velocities in out-of-plane systems with velocities as high as 40 m/s in Co/Ni wires,[7] although the results are still very stochastic. Field-induced DW motion in ultrathin PMA films has been studied extensively during the last decades and it has been shown that the strong DW pinning leads to thermally excited creep motion at low fields. This frustrates the comparison between experimental results and micromagnetic simulations or calculations based on the one-dimensional DW motion model, which has boosted the understanding of DW motion in Py systems. It also has obscured the observation of the so-called Walker breakdown[12] in these ultrathin systems. A major challenge to use the ultrathin PMA films for applications therefore lies in the control of the intrinsic and extrinsic pinning site density and/or strength for DW's. Also fundamentally this has lead to significant progress in the understanding of the interdimensional universality of dynamic interfaces.[13]

In this letter, we show from the dynamics of magnetization reversal that the pinning site density and/or strength for DWs can be significantly reduced using boron-doped Co in Pt/$Co_{100-x}B_x$/Pt. This is tentatively ascribed to a reduction in the amount of grain boundaries due to a change from a polycrystalline state to an amorphous state when adding boron to the magnetic layer. The combination of a high PMA (narrow DWs) and low DW pinning makes Pt/CoB/Pt an interesting candidate for efficient current and field-induced DW motion based devices.

The samples consist of identically prepared Pt(4 nm)/$Co_{100-x}B_x$(0.6 nm)/Pt(2 nm) with $x=0$, 8, 20, and 32 in at. %. The stacks are deposited using dc magnetron sputtering from stoichiometric targets on Si substrates coated with 2 μm SiO_2. A superconducting quantum interference device (SQUID) is used to determine the saturation magnetization and Curie temperature of the films. Polar magneto-optic Kerr effect (MOKE) is used to measure out-of-plane hysteresis loops as function of field sweep rate. The microscopic magnetic domain structure during magnetization reversal was studied with optical Kerr microscopy. All measurements were performed at room temperature.

To determine the magnetic smoothness of the samples and dominant magnetization reversal mechanism we measured DW movement using Kerr microscopy. The magnetization reversal mechanism is investigated by so-called relaxation and remagnetization measurements. In these experiments, the magnetization is first saturated in one direction along the easy axis (out-of-plane) whereafter a small field with opposite polarity is applied. In the remagnetization experiment the field is again switched in polarity during the relaxation allowing us to study the reversibility of the magnetization.[14–17] Figure 1 shows typical magnetization re-

a)Electronic mail: r.lavrijsen@tue.nl.

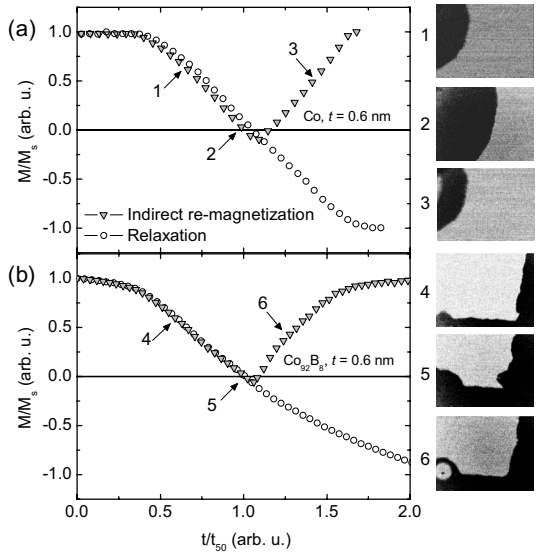

FIG. 1. Example of magnetization relaxation and remagnetization curves plotted against reduced time, the experimental curves are derived from sequences of Kerr microscopy images obtained for a Co sample (a) and (b) $Co_{92}B_8$ sample. Images labeled 1 through 6 are examples of Kerr microscopy images showing the magnetization reversal corresponding to $t/t_{50}=0.5$, 1.0, and 1.3 as indicated in the graph. The black (gray) area correspond to the magnetization pointing up (down) (Dim.: 350×250 μm^2).

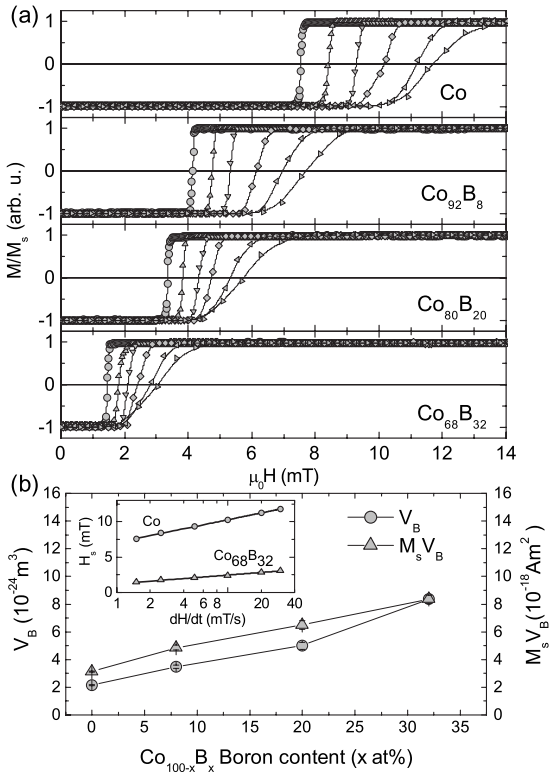

FIG. 2. (a) Partial ($H>0$) hysteresis loops at different field sweep rates $\dot{H}$, increasing from 1.5 mT/s for the circles to 2.5, 5.0, 10, 20, and 30 mT/s for the right pointing triangle, respectively. (b) Barkhausen volume V_B (left scale) and M_sV_B (right scale) as a function of boron content x, the lines are a guide to the eye. The inset shows the switching field as a function of field sweep rate $\dot{H}$ for pure Co and $Co_{68}B_{32}$ as obtained from Fig. 2(a) the solid lines are a fit to Eq. (2).

laxation and remagnetization curves obtained from the reversed area (black/white ratio) of a sequence of Kerr microscopy images of (a) Co and in (b) $Co_{92}B_8$ sample as shown to the right of the graphs. The data is presented as the normalized magnetization at the reduced time t/t_{50}, i.e., the time normalized to the time at which half of the observed area has switched. The shape of the reversal curve reveals information on the magnetic smoothness of the samples and the reversal mechanism.[14,17,18]

In all the reversal experiments we observe a very low DW nucleation site density ($<1/mm^2$) originating from extrinsic inhomogeneities (sample edges and scratches), which is typical for all Co and CoB compositions with a thickness of 0.6 nm. Therefore, we conclude that the magnetization reversal for the 0.6 nm films is dominated by DW motion. On comparing the remagnetization curve with the relaxation curve for both compositions we observe that they are similar in shape and duration (although mirrored) within the experimental limitation (time to reverse the field is finite) and is evidence of reversible DW motion.[17] The reversibility can also be seen on comparing Kerr images 1 and 4 ($t/t_{50}=0.5$) with 3 and 6 ($t/t_{50}=1.3$) which shows that the DW can be moved back and forth in a reversible way.

The reversibility is linked to the magnetic homogeneity which can be associated to the dispersion in the activation energy barrier W, which is related to the DW velocity in the thermally activated (depinning) regime, and can be expressed by[18]

$$v \approx v_0 \exp[-(W-\mu_0 M_s H V_B)/k_B T], \quad (1)$$

where v_0 is a scaling factor, W is the activation barrier height, M_s the saturation magnetization, H the applied field, k_BT the thermal energy, and V_B the Barkhausen volume, i.e., the typical volume that reverses during a single activation event. At this point we like to mention that it is difficult to verify that our experiments are in the depinning regime rather than in the creep regime, which would require the analysis of the DW velocity over many orders of magnitude.[12] Nevertheless, we will use the relaxation measurements to obtain the dispersion σ_w in the activation energy barrier W, fully in line with other studies on similar systems and conditions.[14,17,19] Assuming a square distribution of width σ_w around W, the maximum slope in a reversed magnetization versus $\ln(t)$ plot is equal to $\{-d[M(t)/M_s]/d\ln(t)\}_{max}=k_BT/\sigma_w$.[14] For all our 0.6 nm samples we systematically obtain $\sigma_w=0.12-0.3k_BT$ which is smaller than reported by Bruno *et al.*[14] ($6k_BT$ for Au/Co/Au) and by Czapkiewicz *et al.*[19] ($0.7-1.5k_BT$) for Pt/Co/Pt, showing that the samples exhibit a high magnetic homogeneity.

From Eq. (1) it follows that the DW velocity scales exponentially with M_sV_B in the so-called depinning regime, i.e., $W-\mu_0 M_s H V_B$ produces local energy barriers and thermal activation is needed to overcome this barrier. In this simple description decreasing W and/or increasing M_sV_B would decrease the intrinsic DW pinning. A measure for M_sV_B or W can be found by measuring another manifestation of thermally activated magnetization reversal; the switching field dependence on the field sweep rate. Figure 2(a) shows partial ($H>0$) out-of-plane hysteresis loops at different field sweep rates measured with MOKE for samples with different boron content. First, we notice a significant decrease in the switching field H_s by more than a factor of 6 when increasing the boron concentration up to 32 at. %. Second, for each sample, a clear increase in H_s is observed when the field

sweep rate $\dot{H}$ augments. This behavior can be described for low field sweep rates ($\ll 1$ T/s) in a first order approximation as[14]

$$H_s = \frac{k_B T}{M_s V_B} \times \left\{ \ln(\dot{H}) + \ln\left[\ln(2)\tau_{H=0} \frac{M_s V_B}{k_B T} \right] \right\}, \quad (2)$$

where $\tau_{H=0}$ is the relaxation time at zero field. By fitting the change in H_s versus $\ln \dot{H}$ we obtain $\tau_{H=0}$ and V_B. Note that the derivation of V_B in this way can be interpreted as an effective V_B since it is obtained from a limited range of field sweep rates, without a real physical meaning on an expanded field range. Again, it is not clear if these measurements are taken in the creep or depinning regime, as we discussed before. We are, however, confident that we may compare the obtained (effective) V_B, since we are merely investigating the change in the switching fields and are using a very limited range of field sweep rates as pointed out before. Also the good correspondence of fits to Eq. (2) for all compositions indicates that this interpretation can be used when keeping the above reservations in mind. An example of such a fit to Eq. (2) are given in the inset of Fig. 2(b) for Co and $Co_{68}B_{32}$ showing that H_s indeed varies linearly with $\ln(\dot{H})$. In Fig. 2(b) V_B ($M_s V_B$ on the right scale) is plotted against the boron content x, where we used $M_s = 1420$, 1390, 1320, and 1030 kA/m for $x = 0, 8, 10, 32$, respectively, as obtained from SQUID measurements. A clear increase in V_B and $M_s V_B$ can be seen for increasing boron content. We can translate V_B in a Barkhausen length l_B through $l_B = \sqrt{V_B/d}$ with $d = 0.6$ nm, which can be interpreted as the mean distance between DW pinning sites.[20] This leads to $l_B \approx 60$ nm for pure Co comparable to the results found by Mathet *et al.*[20] on high quality samples and increases to ~118 nm for $Co_{68}B_{32}$, which is nearly a factor two larger. Hence, we obtain a significantly lower pinning site density and/or strength with increasing boron content facilitating DW motion. Please note that a lower Curie temperature T_c will favor easier DW motion. We have estimated T_c from the shape of $M_s(T)$ by SQUID measurements up to 400 K (not shown) as has been done by Vaz *et al.*[21] For all the compositions under study we find $T_c \approx 500 \pm 50$ K indicating that a reduced T_c is not the origin of the increased V_B in the CoB. We speculate that the increase in the distance between pinning centers is due to an increasing amorphous character of the CoB layer when adding boron, thereby decreasing the amount of grain boundaries that are known to be strong pinning sites for DWs.[22] We consider it unlikely that the large increase in V_B could be given by an increase in the DW width Δ with increasing boron doping. The DW width is given by $\Delta = \sqrt{A/K_{eff}}$ where A is the exchange stiffness and K_{eff} the effective perpendicular anisotropy. We have estimated a decrease of K_{eff} between pure Co and $Co_{68}B_{32}$ of 20%. A is, however, hard to determine without making crude assumptions but we speculate that it also decreases with boron doping since the coordination number between Co atoms decreases leaving the DW width almost unchanged. Therefore, we conclude that the addition of boron effectively decreases the amount of pinning sites and/or strength.

In conclusion, the significant decrease in the pinning site density and/or strength together with the high magnetic homogeneity indicates that $Pt/Co_{100-x}B_x/Pt$ has a great potential for efficient current-induced DW motion based devices. Furthermore, the ability to tune the magnetic properties, by choosing the boron doping level, adding Fe and/or change the thickness of the layers, makes it an interesting system for further research.[23] We recently measured a high Gilbert damping ($\alpha \approx 0.2$) in an identically prepared $Pt/Co_{48}Fe_{32}B_{20}/Pt$ sample which might make it possible to measure the Walker breakdown, as a larger damping increases the field at which the Walker breakdown occurs.[23]

We thank NanoNed, a Dutch nanotechnology program of the Ministry of Economic Affairs. Magnetic domain observation was partially supported by network ARTMAG and SPINSWITCH under Contract No. MRTN-CT-2006-035327.

[1] S. S. P. Parkin, M. Hayashi, and L. Thomas, Science **320**, 190 (2008).
[2] D. Allwood, G. Xiong, C. Faulkner, D. Atkinson, D. Petit, and R. Cowburn, Science **309**, 1688 (2005).
[3] M. Kläui, J. Phys.: Condens. Matter **20**, 313001 (2008).
[4] W. C. Uhlig, M. J. Donahue, D. T. Pierce, and J. Unguris, J. Appl. Phys. **105**, 103902 (2009).
[5] G. Tatara and H. Kohno, Phys. Rev. Lett. **92**, 086601 (2004).
[6] J. Xiao, A. Zangwill, and M. Stiles, Phys. Rev. B **73**, 054428 (2006).
[7] T. Koyama, G. Yamada, H. Tanigawa, S. Kasai, N. Ohshima, S. Fukami, N. Ishiwata, Y. Nakatani, and T. Ono, Appl. Phys. Express **1**, 101303 (2008).
[8] D. Ravelosona, D. Lacour, J. Katine, B. Terris, and C. Chappert, Phys. Rev. Lett. **95**, 117203 (2005).
[9] O. Boulle, J. Kimling, P. Warnicke, M. Klaui, U. Rudinger, G. Malinowksi, H. Swagten, and B. Koopmans, Phys. Rev. Lett. **101**, 216601 (2008).
[10] D. Ravelosona, S. Mangin, J. Katine, E. Fullerton, and B. Terris, Appl. Phys. Lett. **90**, 072508 (2007).
[11] I. Miron, P. Zermatten, G. Gaudin, S. Auffret, B. Rodmacq, and A. Schuhl, Phys. Rev. Lett. **102**, 137202 (2009).
[12] P. J. Metaxas, J. P. Jamet, A. Mougin, M. Cormier, J. Ferre, V. Baltz, B. Rodmacq, B. Dieny, and R. L. Stamps, Phys. Rev. Lett. **99**, 217208 (2007).
[13] K.-J. Kim, J.-C. Lee, S.-M. Ahn, K.-S. Lee, C.-W. Lee, Y. J. Cho, S. Seo, K.-H. Shin, S.-B. Choe, and H.-W. Lee, Nature (London) **458**, 740 (2009).
[14] P. Bruno, G. Bayreuther, P. Beauvillain, C. Chappert, G. Lugert, D. Renard, J. Renard, and J. Seiden, J. Appl. Phys. **68**, 5759 (1990).
[15] J. Ferré, V. Grolier, P. Meyer, S. Lemerle, A. Maziewski, E. Stefanowicz, S. Tarasenko, V. Tarasenko, M. Kisielewski, and D. Renard, Phys. Rev. B **55**, 15092 (1997).
[16] M. Kisielewski, A. Maziewski, M. Tekielak, J. Ferre, S. Lemerle, V. Mathet, and C. Chappert, J. Magn. Magn. Mater. **260**, 231 (2003).
[17] M. Czapkiewicz, T. Stobiecki, and S. van Dijken, Phys. Rev. B **77**, 024416 (2008).
[18] M. Labrune, S. Andrieu, F. Rio, and P. Bernstein, J. Magn. Magn. Mater. **80**, 211 (1989).
[19] M. Czapkiewicz, J. Kanak, T. Stobiecki, M. Kachel, M. Zoladz, I. Sveklo, A. Maziewski, and S. van Dijken, Mater. Sci. (Poland) **26**, 839 (2008).
[20] V. Mathet, T. Devolder, C. Chappert, J. Ferre, S. Lemerle, L. Belliard, and G. Guentherodt, J. Magn. Magn. Mater. **260**, 295 (2003).
[21] C. Vaz, J. Bland, and G. Lauhof, Rep. Prog. Phys. **71**, 056501 (2008).
[22] S. Lemerle, J. Ferre, C. Chappert, V. Mathet, T. Giamarchi, and P. Le Doussal, Phys. Rev. Lett. **80**, 849 (1998).
[23] G. Malinowski, K. C. Kuiper, R. Lavrijsen, H. J. M. Swagten, and B. Koopmans, Appl. Phys. Lett. **94**, 102501 (2009).